Supporting Information

Gerlic et al. 10.1073/pnas.1215995110

SI Materials and Methods

Reagents, Chemicals, and Antibodies. Cell-culture supplies were obtained from Gibco. The following antibodies were used for immunoblotting according to standard protocols: anti-Flag M2 (Sigma), anti-c-Myc (Roche), anti-human IL-1β (R&D Systems). The anti-GST, anti-GFP (B-2), anti-mouse caspase-1 protein (p)10 (M-20), anti-human caspase-1 p10 (C-20) and p20 (C-15) antibodies were purchased from Santa Cruz Biotechnology. Antibodies against the viral proteins F1L and N1L were produced in rabbits by immunization with F1L peptide as described (1), or with purified N1L protein produced in *Escherichia coli*. Muramyl dipeptide (MDP) was purchased from InvivoGen or Alexis for either cell-based or in vitro studies. Lipopolysaccharide (LPS) was obtained from Alexis, and N-acetyl-Trp-Glu-His-Asp-AMC (7-amino-4-methylcoumarin) (Ac-WEHD-AMC), N-acetyl-Trp-Glu-His-Asp-rhodamine-D112 (Dansyl ethylenediamine) (Ac-WEHD-RhoD112), and Ac-WEHD-CHO were obtained from Calbiochem.

Plasmids. Plasmids encoding Flag-Caspase-1, ProIL-1β, Myc-apoptosis-associated speck-like protein containing a caspase recruitment domain (ASC), Flag/Myc-pyrin domain containing protein (NLRP) 1, Myc-nucleotide–binding oligomerization domain-containing protein 2 (NOD2), GFP-F1L, -Δ44 and -Δ57–78 were described (1, 2). Recombinant baculovirus transfer vectors encoding human NLRP1, pro-Caspase-1 (p45) or NLRP1Δleucine-rich repeat (LRR) mutant (retains 1–723/1236–1473 amino acids) were described (3).

GST Pull-Down. Recombinant proteins were produced by baculovirus infection of nucleotide-binding oligomerization domain, leucine-rich repeat and Spodoptera frugiperda (Sf9) insect cells (GST-NLRP1, GST-NLRP1ΔLRR) or in bacteria [GST–BCL2-related protein A1 (Bfl-1), GST-F1L, or GST] as described (3, 4). Various proteins were mixed (5 μg) with or without purified F1L protein (10 μg) in 20 mM Hepes-KOH at pH 7.5, 10 mM KCl, and 1 mM DTT in a final volume of 50 μL for 30 min on ice, followed by incubation overnight with glutathione-sepharose at 4 °C. GST-purified complexes were isolated after centrifugation, washed, and eluted with SDS-loading buffer, then analyzed by SDS/PAGE and stained by Sypro Ruby.

In Vitro Reconstituted NLRP1 Inflammasome. The in vitro reconstitution of the NLRP1 inflammasome using proteins expressed in Sf9 cells from recombinant baculoviruses has been described (3). Briefly, reactions contained 8.5 nM His_6-NLRP1, 8.5 nM procaspase-1, 0.25 mM ATP, 0.5 mM Mg^{2+}, 0.1 μg/mL MDP and GST-B-cell CLL/lymphoma 2 (Bcl-2) or N1L, wild-type or various mutants of recombinant 17 nM GST-F1L, or various synthetic peptides. Caspase-1 activity was measured after 60 min by hydrolysis of Ac-WEHD-AMC substrate (20 μM), expressing data as mean ± SD, $n = 3$.

Caspase-1 Processing in the Reconstituted NLRP1 Inflammasome. Reactions contained 0.1 μM His_6-NLRP1 or GST-NLRP1ΔLRR, 0.1 μM procaspase-1, 1 mM ATP, 1 mM Mg^{2+}, 10 μg/mL MDP and recombinant GST-F1L 1–47 protein or synthetic F1L 22–47 peptide (F1Lp), or 0.4 μM recombinant N1L and were incubated 30 min at 37 °C. Proteins were separated by SDS/PAGE and analyzed by immunoblotting using anti-p10 caspase-1 antibodies in conjunction with secondary IRDye 800/680CW-conjugated antibodies (LI-COR Biosciences). Results were imaged by using Li-COR Odyssey v3.0 software.

Analysis of ATP Binding to NLRP1 by fluorescence polarization assay. His_6-NLRP1 (0.125 μM) was incubated for 5 min on ice in the presence of F1L 1–47 (2 μM), 0.5 or 2 μM F1Lp 22–47, N1L, F1Lp 32–37, or 2 μM Bcl-2p 41–60. The mixture was then incubated for an additional 5 min in ice with 1 μM MDP-LD, 10 nM fluorescein-conjugated ATP analog and 0.5 mM Mg^{2+}. ATP binding was analyzed by fluorescence polarization assay (FPA) [measuring milliPolars (mP)] using an Analyst AD Assay Detection System (LJL Biosystem), and the percentage of inhibition was determined compared with NLRP1 incubated only with MDP-LD (mean ± SD).

Peptide Synthesis and Purification. Peptides were synthesized by using Rink Amide ChemMatrix resin (Matrix Innovation) using Fmoc synthesis and diisopropylcarbodiimide/1-hydroxybenotiazde (DIC/HOBt) coupling with an Advanced ChemTech Apex 396 multiple peptide synthesizer. Peptides were cleaved from the resin by using standard cleavage and deprotection conditions and purified by HPLC on a Phenomenex Luna C18 column (250 × 21.2 mm, 5 μm). Purified peptides were all single peaks (>99% purity) by analytical HPLC, and their mass was confirmed by MALDI mass spectroscopy.

Cell Culture. HeLa and 293T cells were cultured in DMEM supplemented with 10% FBS and antibiotics. Human acute monocytic leukemia cell line (THP-1), THP-1-Blue, and PBMC were cultured in complete RPMI medium 1640 10% FBS and antibiotics. For differentiation, THP-1 cells were stimulated for 18 h with 50 ng/mL phorbol-12-myristate-13-acetate. PBMC used in infection studies were obtained from healthy donors (San Diego Blood Bank) and isolated by density-gradient centrifugation using Ficol.

Vaccinia Virus Production. The revertant F1L viruses (Flag-F1L and Flag-F1L(N32A, H35A) were generated by introducing wild-type or mutant F1L genes in frame with a pE/L-Cherry selection cassette. The ΔN1L virus was generated by replacing nucleotides 1–275 of the N1L open reading frame 63 (Orf63) with a pE/L-gpt-Cherry selection cassette. The fidelity of the resulting recombinant viruses was verified by DNA sequencing. Expression of the Flag-F1L proteins and loss of expression of N1L was documented by immunoblot analysis of infected cells. The Vaccinia virus (VACV) strains were grown in HeLa cells and titered on VeroE6 cells.

VACV Infection of Cultured Cells. 12-D-tetradecanoylphorbol-13-acetate (TPA)-differentiated THP-1 cells were infected at various multiplicities of infection (MOI) with VACV-Western Reserve (WR), N1L deleted virus (ΔN1L), or F1L deleted virus (ΔF1L).

Intracellular Staining for E3L Viral Antigen. VACV-infected THP-1 cells (as above) were collected 18 h after infection. Cells were fixed with cytofix-cytosperm (BD Biosciences) for 20 min at 4 °C. Fixed cells were subjected to intracellular E3L staining in Perm/Wash buffer (BD Biosciences) for 30 min at 4 °C. Anti-E3L Ab was kindly provided by Shane Crotty (La Jolla Institute for Allergy and Immunology) and used at a 1:100 vol/vol dilution. Cells were washed twice with BD Perm/Wash buffer and stained with goat anti-mouse IgG biotin-conjugated antibody at 4 °C followed by addition of PE-conjugated streptavidin (BD Biosciences). Samples were analyzed for proportion of intracellular E3L staining

after gating on live cells using a FACSCalibur flow cytometer with CellQuest (BD Biosciences) and FlowJo software (Tree Star).

NF-κB Activation in THP-1-Blue Cells. Using THP-1-Blue cells (ATCC; InvivoGen), NF-κB activation was evaluated by measuring alkaline phospatase activity in the supernatant for 180 min by hydrolysis of QUANTI-Blue substrate (InvivoGen). As a positive control, THP-1 macrophages were stimulated for 18 h with MDP (5 μg/mL). Reported results are mean ± SD; $n = 3$.

Immunoblot Analysis. Immunoblot analysis of cell extracts was performed by standard methods. For immunoblot analysis of culture supernatants, the recovered fluids were filtered by using an Amicon Ultra (100 kDa cutoff). Proteins contained in eluates were precipitated by trichloroacetic acid and washed twice with acetone. Dry pellets were resuspended in 2× Laemmli buffer, normalized by the amount of total protein, separated by SDS/PAGE, and analyzed by immunoblotting using various antibodies in conjunction with secondary IRDye 800/680CW-conjugated antibodies (LI-COR Biosciences). Results were imaged by using Li-COR Odyssey v3.0 software and quantified by integrated fluorescence intensity.

Coimmunoprecipitations. HEK293T cells were transiently cotransfected with plasmids encoding Myc or flag-tagged NLR full-length proteins and either GFP-tagged N1L or GFP-tagged F1L. For coimmunoprecipitations, 5×10^5 to 1×10^6 cells were lysed in isotonic, Nonidet P-40–containing lysis buffer (150 mM NaCl, 20 mM Hepes at pH 7.4, 0.2% Nonidet P-40, 5 mM $MgCl_2$, 2 mM EDTA, 2 mM DTT, 1 mM PMSF, and 1× protease inhibitor mix (Roche). Clarified lysates were subjected to immunoprecipitation (IP) by using Dynabeads proteinG (Invitrogen) conjugated with anti-GFP, -Myc, or -flag antibodies. After overnight incubation at 4 °C, immune complexes were washed three times in lysis buffer, separated by SDS/PAGE, and analyzed by immunoblotting using various antibodies in conjunction with secondary IRDye 800/680CW-conjugated antibodies (LI-COR Biosciences). Results were imaged by using Li-COR Odyssey v3.0 software and quantified by integrated fluorescence intensity. Where indicated, cell lysates (10% volume) were run directly in SDS gels.

Confocal Microscopy. HeLa cells were grown overnight on Lab-Tek II coverslip chambers and cotransfected with plasmids encoding F1L-GFP and Myc-NLRP1 by using jetPRIME. After 24 h, cells were fixed with 4% (kg/dL) formaldehyde, permeabilized with PBS + 0.3% (vol/vol) Triton X-100 for 10 min, and blocked with PBS + 3% BSA for 30 min. Cells were immunostained with anti-Myc antibody (Sigma; 1:200) overnight, then washed with PBS and incubated with Alexa Fluor 594-conjugated secondary antibody (1:200 vol/vol) for 1 h. Cells were washed with PBS, and coverslips were mounted by using Vectashield. Images were acquired by confocal laser-scanning microscopy using a LSM 710 NLO Zeiss Multiphoton Laser Point Scanning Confocal Microscope equipped with a 63× objecting using inverted-based microscopy.

Mice. The studies reported here conform to the animal Welfare Act and followed National Institutes of Health guidelines for the care and use of animals in biomedical research. All experiments were performed in compliance with the regulations of the La Jolla Institute Animal care committee in accordance with the guidelines set by the Association for assessment and Accreditation of laboratory Animal Care. Eight- to 12-wk-old female BALB/c mice were purchased from the Jackson Laboratory. Animal experiments were approved by Sanford-Burnham Medical Research Institutional Animal Care and Use Committee (IACUC).

VACV Intranasal Challenge. Eight- to 12-wk-old female BALB/c were anesthetized by inhalation of isoflurane and inoculated by the intranasal route with VACV, Western Reserve (VACV-WR), and a mutant of WR in which only the F1L gene was deleted, VACV-F1L (10^4 or 10^5 pfu per mice). Body weight and rectal temperature of mice were measured daily before and after infection. At various times after infection, four mice from each group were killed and lungs and BAL fluids were collected. Mice were euthanized when they lost 30% of their initial body weight or were severely hypothermic (<32 °C) on two consecutive days.

Bronchoalveolar Lavage. Lungs were lavaged with 0.5 mL of PBS containing 2% BSA. The recovered bronchoalveolar lavage (BAL) fluids were centrifuged to pellet cells. The supernatants (500 μL) were concentrated 10× by using an Amicon Ultra (3-kDa cutoff). Proteins contained in eluates were mixed with 5× Laemmli buffer, separated by SDS/PAGE, and analyzed by immunoblotting using anti-mouse caspase-1 p10 (M-20) in conjunction with secondary IRDye 800/680CW-conjugated antibodies (LI-COR Biosciences). Results were imaged by using Li-COR Odyssey v3.0 software and quantified by the integrated fluorescence intensity.

Characterization of Lung Histology. Lungs were removed after killing animals, fixed in 10% zinc-buffered formalin (Protocal; Fisher Diagnostics), and embedded in paraffin. Deparaffinized 5-μm-thick sections were stained with hematoxylin and eosin for histopathological assessment. All slides were scanned at an absolute magnification of 400× (resolution of 0.25 μm per pixel) by using the Aperio ScanScope CS system (Aperio Technologies). The acquired digital images representing whole-tissue sections were viewed and analyzed by using the ImageScope viewer. To quantify foci of inflammation in lung sections, focal areas of peribronchial and perivascular inflammation were selected with the pen tool. Mean and SEM values for numbers of foci were determined. Lung sections were analyzed by the terminal deoxynucleotidyl transferase end-labeling (TUNEL) method (Chemicon International) to identify the DNA fragmentation of apoptotic cells. The percentage of TUNEL-positive cells was evaluated by a morphometric method using an automated image analysis system (Aperio Technologies) and applying a nuclear scoring algorithm (5).

Statistics. In vivo data are presented as mean ± SEM. All other data were presented as the mean ± SD from at least three independent experiments. Statistical comparisons between different treatments were performed by two-tailed Student's t test, two-way ANOVA, log-rank analysis, or Bonferroni's test, using PRIZM software.

1. Postigo A, Cross JR, Downward J, Way M (2006) Interaction of F1L with the BH3 domain of Bak is responsible for inhibiting vaccinia-induced apoptosis. *Cell Death Differ* 13(10): 1651–1662.
2. Bruey JM, et al. (2007) Bcl-2 and Bcl-XL regulate proinflammatory caspase-1 activation by interaction with NALP1. *Cell* 129(1):45–56.
3. Faustin B, et al. (2007) Reconstituted NALP1 inflammasome reveals two-step mechanism of caspase-1 activation. *Mol Cell* 25(5):713–724.
4. Yu E, et al. (2011) Structural determinants of caspase-9 inhibition by the vaccinia virus protein, F1L. *J Biol Chem* 286(35):30748–30758.
5. Krajewska M, et al. (2009) Image analysis algorithms for immunohistochemical assessment of cell death events and fibrosis in tissue sections. *J Histochem Cytochem* 57(7): 649–663.

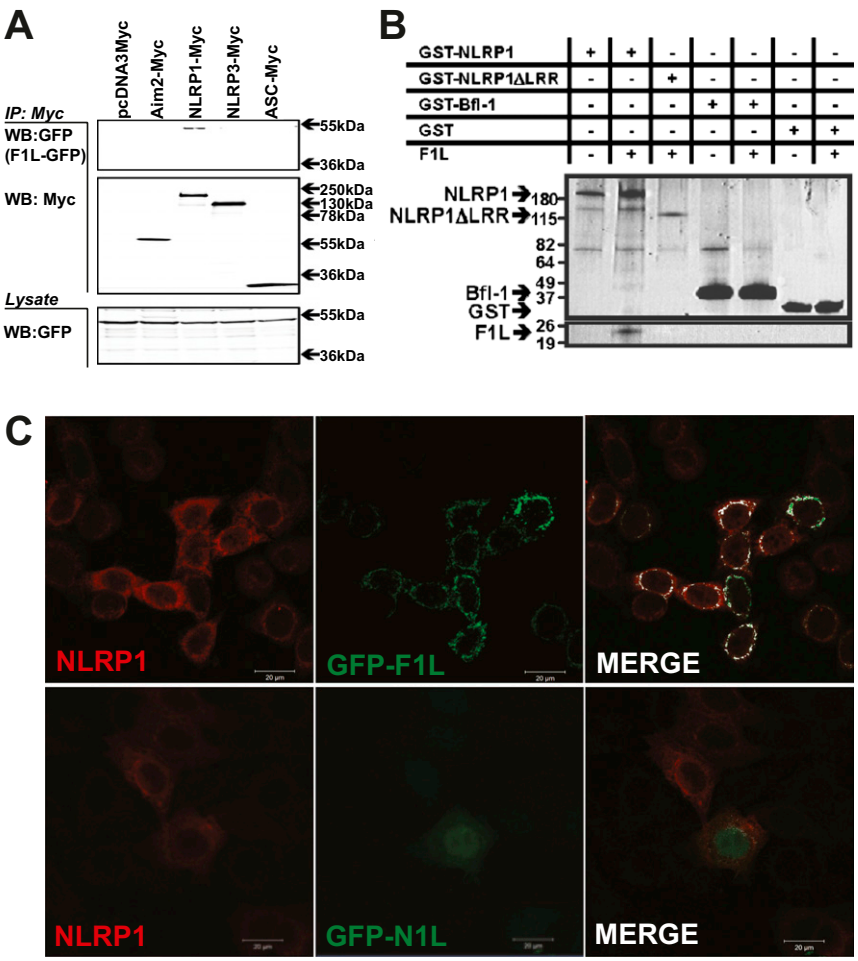

Fig. S1. Studies of F1L binding to NLRP1. (*A*) HEK293T cells were transiently cotransfected with plasmids encoding various Myc-tagged proteins and GFP-tagged F1L (empty Myc plasmid served as negative control). For coimmunoprecipitations (co-IPs), ~10^6 cells were lysed in isotonic Nonidet P-40 lysis buffer and lysates were normalized for protein content. Clarified lysates were subjected to IP by using protein-G anti-GFP. Immune complexes were separated by SDS/PAGE and analyzed by immunoblotting using anti-Myc and anti-GFP antibodies using a fluorescence-based imaging system (*Top* and *Middle*). Cell lysates (5% volume) were also run alongside immune complexes (*Bottom*). (*B*) Recombinant proteins GST-NLRP1, GST-NLRP1ΔLRR, GST-Bfl-1, or GST (5 μg) were incubated with or without purified F1L (10 μg) in 20 mM Hepes-KOH at pH 7.5, 10 mM KCl, and 1 mM DTT in a final volume of 50 μL for 30 min on ice, followed by incubation overnight with glutathione-sepharose at 4 °C. GST-purified complexes were isolated after centrifugation, analyzed by SDS/PAGE, and stained with Sypro Ruby. All data are representative of at least three independent experiments. F1L peptides inhibit NLRP1. Various F1L peptides (F1Lp) or recombinant GST-F1L 1–47 protein (50 nM) were added to in vitro reconstituted NLRP1 inflammasome. (*C*) NLRP1 colocalizes with F1L in cells. Confocal fluorescence microscopy analysis was performed on HeLa cells cotransfected with plasmids encoding Myc-NLRP1 and either GFP-F1L (*Upper*) or GFP-N1L (*Lower*). Cells were immunostained by using anti-Myc antibody for detection of Myc-NLRP1 (red). Colocalization of NLRP1 (red) and F1L (green) was evaluated by using ImageJ software, displaying merged fluorescence as white color (*Right*). Note punctate (presumably mitochondrial) colocalization of NLRP1 with GFP-F1L in cytosol of cells, in contrast to lack of NLRP1 colocalization with GFP-N1L protein.

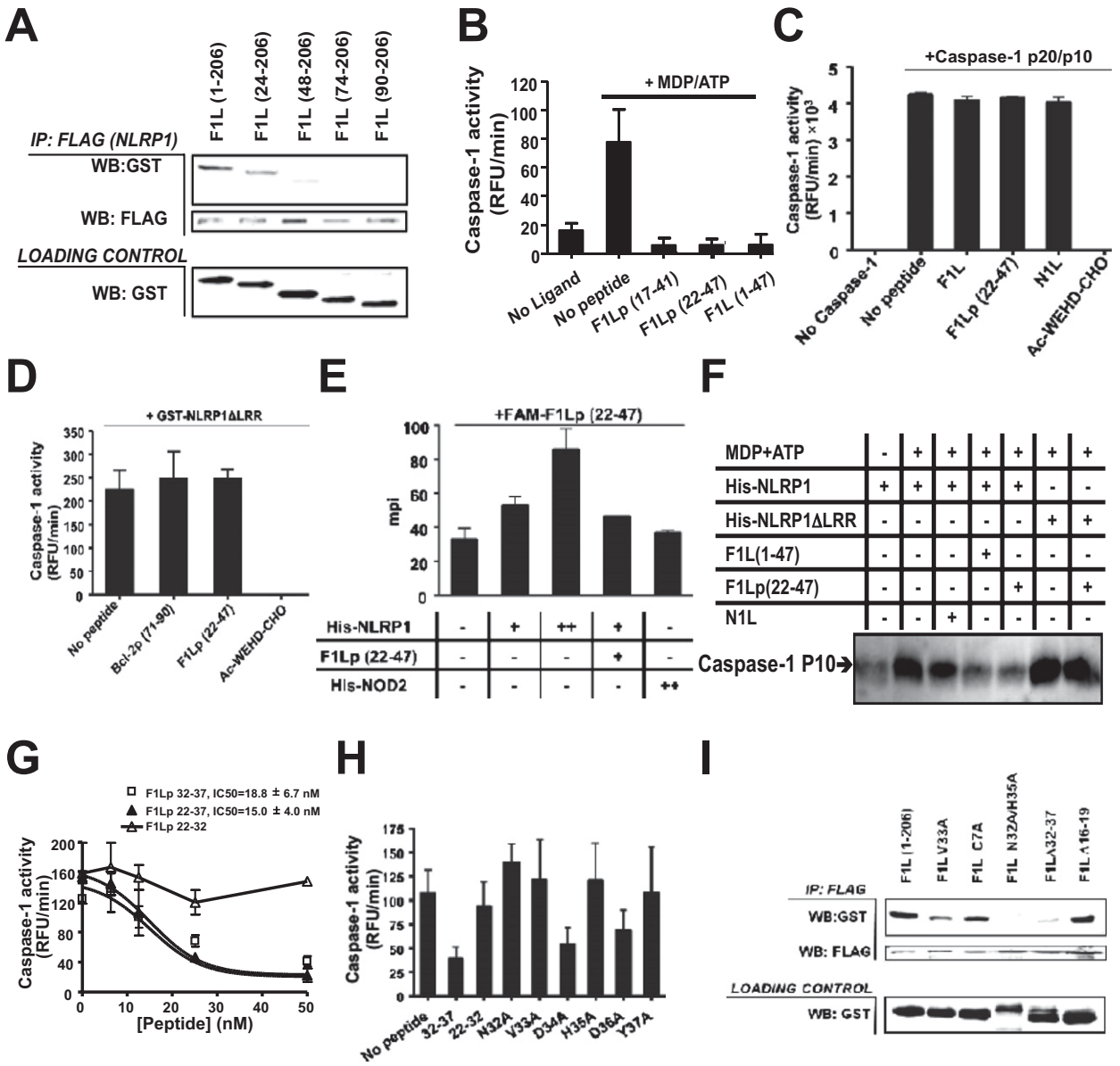

Fig. S2. (*A*) HEK293T cells were transiently transfected with plasmid encoding Flag-tagged NLRP1 and lysates were prepared, to which were added various GST-F1L proteins as indicated. Samples were subjected to IP by using protein-G anti-Flag. Immune complexes (*Top* and *Middle*) and GST-tagged recombinant proteins (2 μg) (*Bottom*) were analyzed by SDS/PAGE immunoblotting using anti-GST or anti-Flag antibodies. (*B–D* and *H*) In vitro reconstituted NLRP1 inflammasome was used to study F1L activity. Reactions contained 8.5 nM His_6-NLRP1, 8.5 nM procaspase-1, 0.25 mM ATP, 0.5 mM Mg^{2+}, 0.1 μg/mL MDP, and 17 nM GST-Bcl-2, N1L, or various GST-F1L constructs. Caspase-1 activity was measured by hydrolysis of 20 μM Ac-WEHD-AMC substrate. (*B*) F1L peptide (22–47) suppresses NLRP1-induced proteolytic processing of procaspase-1 in vitro. (*C*) Recombinant, purified active (p10/p20 heterodimer) 5 nM Caspase-1 was incubated with or without 50 nM GST-F1L, F1Lp 22–47, or N1L, or with 10 nM Ac-WEHD-CHO. Caspase-1 activity was measured after 60 min by hydrolysis of 20 μM Ac-WEHD-AMC substrate, expressing data as mean ± SD, $n = 3$. (*D*) Reactions contained 8.5 nM GST-NLRP1ΔLRR, 8.5 nM pro-Caspase-1, 0.25 mM ATP, 0.5 mM $MgCl_2$, with 0.1 μg/mL MDP, with or without 50 nM Bcl-2p 71–90, 50 nM F1Lp 22–47, or 10 nM Ac-WEHD-CHO. Caspase-1 activity was measured after 60 min by hydrolysis of Ac-20 μM WEHD-AMC substrate, expressing data as mean ± SD, $n = 3$. (*E*) His_6-NLRP1 at 0.5 μM (+) or 2 μM (++) or His_6-NOD2 at 2 μM (++) was incubated for 5 min on ice with (+) or without (-) unlabeled F1Lp 22–47 peptide (1 M Hepes, pH 7.4). Then, 0.1 μM carboxyfluorescein (FAM)-conjugated F1L 22–47 peptide (F1lp22-47) was added for 5 min at 4 °C. Binding of fluorochrome-labeled peptide was analyzed by FPA, measuring milliPolars (mP), mean ± SD ($n = 3$). (*F*) Reactions contained His_6-NLRP1 or GST-NLRP1ΔLRR, procaspase-1, and $MgCl_2$, with (+) or without (-) ATP and MDP and with or without of recombinant GST-F1L(1-47) or GST-N1L proteins or synthetic F1L peptide (22-47) [F1Lp(22-47)]. After incubation for 30 min at 37 °C, proteins were separated by SDS/PAGE and analyzed by immunoblotting using anti-p10 caspase-1 antibody. See Fig. S1 for more information. (*G*) Concentration-dependent suppression of NLRP1 by F1L. Various concentrations of F1Lp32-37, F1Lp22-37, or F1Lp22-32 were added to in vitro reconstituted NLRP1 inflammasome. Caspase-1 activity was measured, and IC_{50} values were calculated. See Fig. S1 for more information. (*H*) Alanine scanning substitution analysis of F1L peptides. Various F1Lp 32–37 peptides where specific residues were replaced by 50 nM L-Ala were added to in vitro reconstituted NLRP1 inflammasome and analyzed as above. (*I*) HEK293T cells were transiently transfected with plasmid encoding Flag-tagged NLRP1 and lysates were prepared, to which were added various GST-F1L proteins as indicated. Samples were subjected to IP by using protein-G anti-Flag. Immune complexes were analyzed by SDS/PAGE immunoblotting using anti-GST or anti-Flag antibodies (*Top* and *Middle*). GST-tagged recombinant proteins (2 μg) were run directly in gels as a control for loading (*Bottom*).

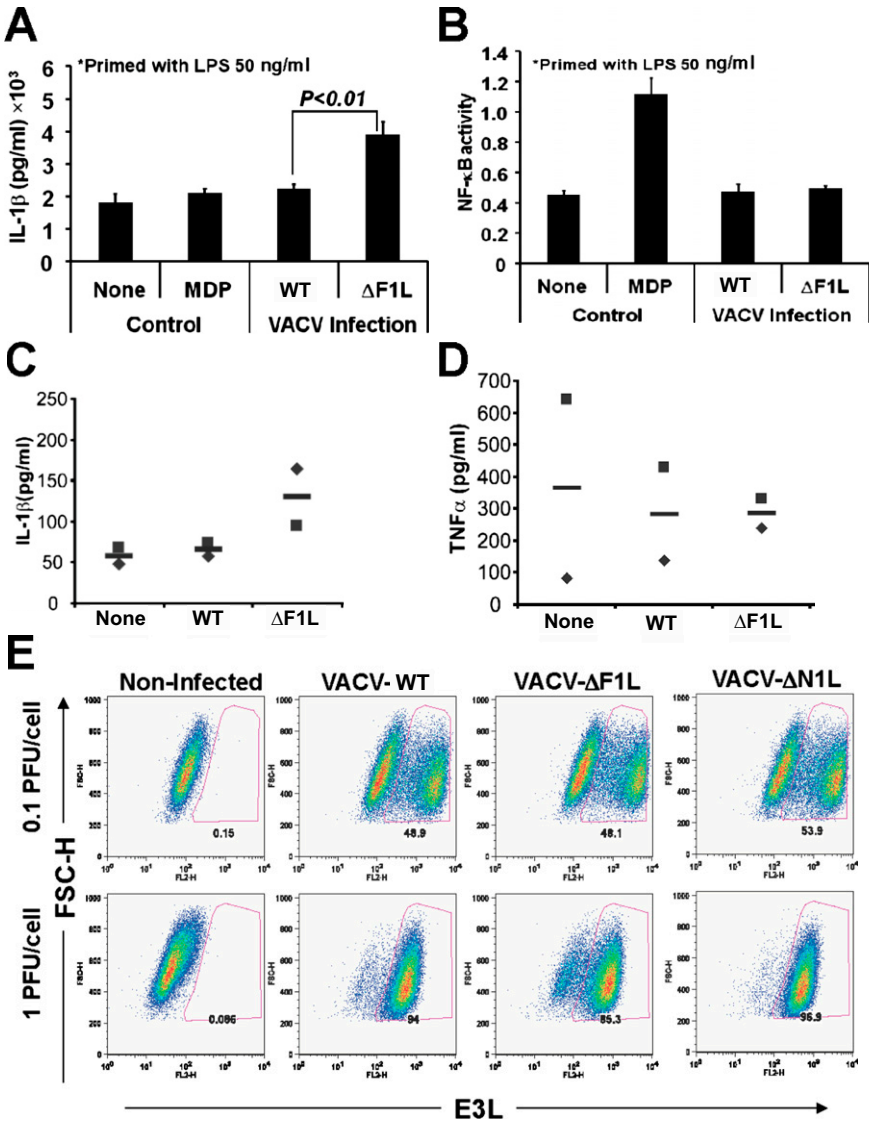

Fig. S3. F1L inhibits IL-1β secretion by LPS-primed, VACV-infected macrophages. (*A* and *B*) TPA-differentiated THP-1-Blue cells (10^6) were primed 12 h with 50 ng/mL LPS, followed by infection (MOI = 1) with VACV WR (WT) or VACV ΔF1L viruses. Supernatants were collected 18 h later for analysis. IL-1β secretion (*A*) was measured by using ELISA, and NF-κB activity (*B*) was measured by alkaline phospatase reporter gene assays. As positive control for *A* and *B*, macrophages were stimulated for 18 h with 5 μg/mL MDP. All results are mean ± SD; n =3. (*C* and *D*) PBMC were collected from two donors by using Ficol density gradient centrifugation and cultured overnight. PBMC were then primed with 10 pg/mL LPS for 18 h before infection with wild-type VACV (WT) or F1L deleted virus (ΔF1L) (MOI = 1). IL-1β (*C*) and TNFα (*D*) secretion were measured by ELISA (eBioscience) (n = 2). Hash marks indicate mean values. (*E*) Deletion of F1L or N1L does not impair infection efficiency of VACV in THP-1 cells. TPA-differentiated THP-1-Blue (InvivoGen) cells (10^6) were infected (MOI = 0.1 and 1) with wild-type VACV-WR, F1L deleted virus (ΔF1L), or N1L deleted virus (ΔN1L). Cells were collected, permeabilized, and stained by using antibody recognizing the VACV early gene E3L, followed by flow cytometry analysis. Data represent fluorescence intensity (*x* axis) versus forward scatter (*y* axis), where each cell analyzed appears as a dot and values are color coded on the visible light spectrum to indicate low (blue) versus high (red) frequency values. The demarked areas represent immunopositive cells, where the percentage of E3L-expressing cells is provided in each graph.

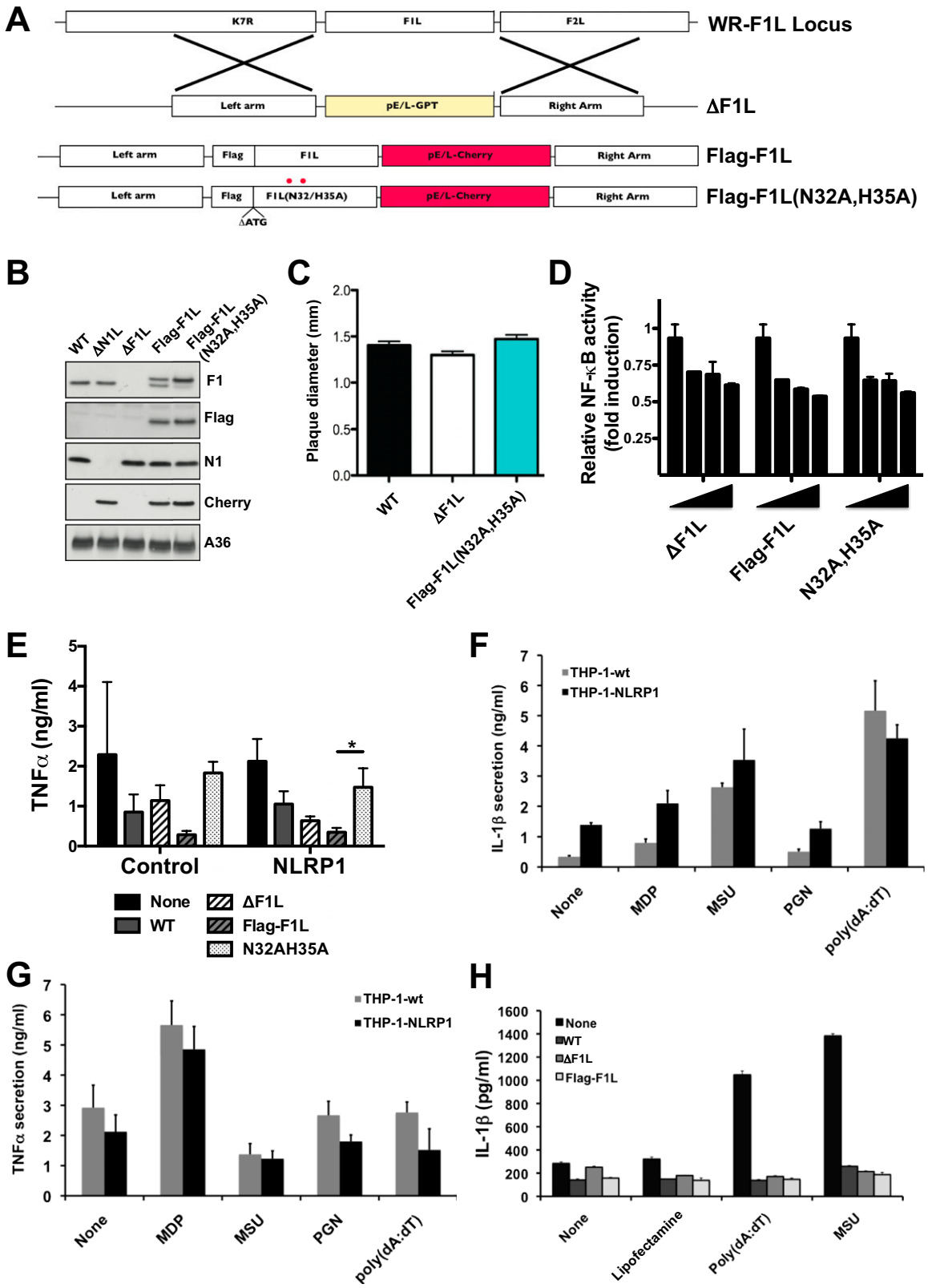

Fig. S4. Studies with recombinant virus encoding non-NLR binding F1L mutant. (*A*) Schematic presentation of VACV mutant strains used in this work. (*B*) HeLa cells were infected (MOI = 1) for 6 h with the wild-type VACV Western Reserve (WR) or various VACV F1L mutants. Levels of F1L, N1L, Flag, Cherry Red Protein, and A36 (loading control) proteins were assessed by immunoblotting using cell lysates normalized for total protein content. (*C*) Plaque sizes in monolayers of cell culture produced by infection with VACV ΔF1L and Flag-F1L (N32A,H35A) were compared with VACV wild-type (WT). (*D*) TPA-differentiated THP-1-Blue (InvivoGen) cells (10^6) were infected (MOI = 0.5–5) with VACV ΔF1L, Flag-F1L, or Flag-F1L(N32A,H35A) viruses. NF-κB activity was measured by alkaline phospatase reporter gene assays. Data are mean ± SD ($n \geq 3$). (*E* and *F*) Analysis of the NLRP1 stably overexpressing THP-1-Blue cells. The 10^6 TPA-differentiated

Legend continued on following page

THP-1-Blue cells (THP-1-wt) and NLRP1 stably overexpressing THP-1-Blue (THP-1-NLRP1) were primed 12 h with 50 ng/mL LPS, followed by different inflammasome activating agents [e.g., MDP, monosodium urate (MSU), PGN, poly(dA:dT)]. Supernatants were collected and analyzed for IL-1β (*E*) and TNFα (*F*) secretion by using ELISA (mean ± SD; $n = 3$). (*G*) TPA-differentiated THP-1-Blue (InvivoGen) cells (10^6) were primed 12 h with LPS (50 ng/mL), followed by infection (MOI = 1) with VACV WT, VACV ΔF1L, and Flag-F1L viruses for 2 h. Macrophages were stimulated for 6 h with Poly(dA:dT) (1 μg/mL) or MSU (50 μg/mL). Supernatants were collected 6 h later for analysis of IL-1β levels by ELISA. Data represent mean ± SD ($n = 3$). (*H*) NLRP1 overexpressing or control transfected THP-1 cells were infected at MOI = 2, and culture supernatants were analyzed 16 h later for TNFα by ELISA (mean ± SD; $n \geq 3$). Statistical significance at the level of $P < 0.05$ is indicated by asterisk.

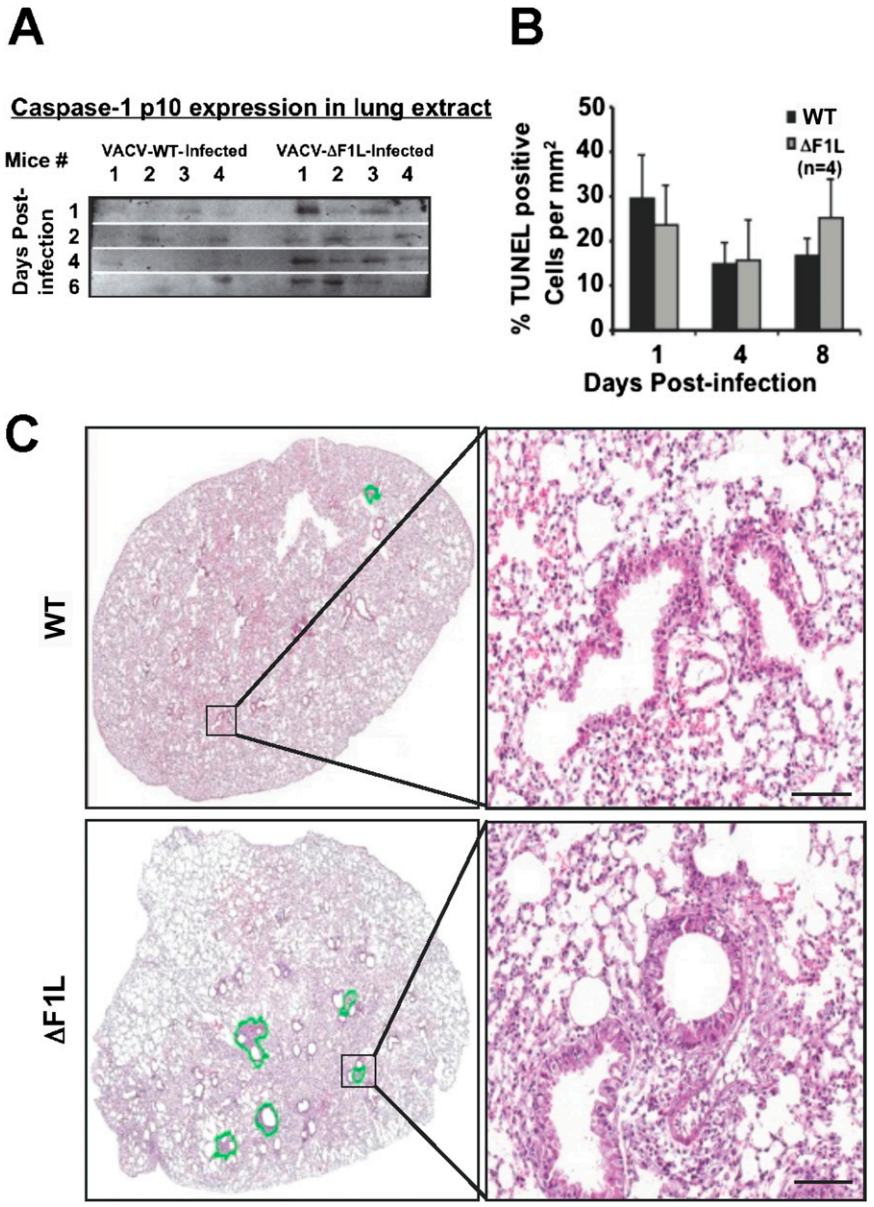

Fig. S5. In vivo studies of recombinant VACV in mice. Mice were infected intranasally with 10^4 ($n = 6$–8 mice per group) or 10^5 ($n = 30$ mice per group) pfu of wild-type VACV (WT) or F1L deleted virus (ΔF1L), (Fig. 4 *B*–*G*). At various days after infection, four mice from each group were killed and BAL fluids were collected from mice infected with WT or F1L-deficient viruses, 10× concentrated, and analyzed by SDS/polyacrylamide gel electrophoresis (PAGE) immunoblotting for caspase-1 cleavage using anti-p10 antibody (*A*). Apoptosis in lungs of the above killed mice was analyzed (*B*) by the TUNEL staining of five lung tissue sections. Lungs data represent mean ± SEM ($n = 4$). (*C*) Histology of lungs in VACV murine intranasal model. BALB/c mice ($n = 4$) were infected intranasally with 10^5 pfu of WT VACV or mutant virus (ΔF1L). Lungs were harvested on day 4 after infection. Deparaffinized 5-μm-thick sections were stained with hematoxylin/eosin for histopathological assessment. All slides were scanned at an absolute magnification of 400× (resolution of 0.25 μm per pixel) by using the Aperio ScanScope CS system (Aperio Technologies). The acquired digital images representing whole-tissue sections were viewed and analyzed by using the ImageScope viewer. Foci of inflammation in lung sections were quantified by selecting with the pen tool (green line) focal areas of peribronchial and perivascular inflammation. Pen tool annotations (green line) denote foci of inflammation of day 4 after infection. Representative low (*Left*) and high (*Right*) power magnification images are shown, where boxes show regions selected for high-power magnification imaging. (Scale bars: 100 μm.)

Table S1. F1L peptides tested in this study

Peptide length	Amino acid sequence
25′mers	
7–31	CNNIVDYVDDIDNGIVQDIEDEASN
12–36	DYVDDIDNGIVQDIEDEASNNVDHD
17–41	IDNGIVQDIEDEASNNVDHDYVYPL
22–47	VQDIEDEASNNVDHDYVYPLPENMVY
Short peptides	
22–42	VQDIEDEASNNVDHDYVYPLP
22–37	VQDIEDEASNNVDHDY
22–32	VQDIEDEASNN
27–37	DEASNNVDHDY
32–37	NVDHDY
22–35	VQDIEDEASNNVDH
22–34	VQDIEDEASNNVD
22–33	VQDIEDEASNNV
Alanine substituted 6′mers	
N32A	AVDHDY
V33A	NADHDY
D34A	NVAHDY
H35A	NVDADY
D36A	NVDHAY
Y37A	NVDHDA
FAM labeled peptides	
7–31	FAM-CNNIVDYVDDIDNGIVQDIEDEASN
12–36	FAM-DYVDDIDNGIVQDIEDEASNNVDHD
17–41	FAM-IDNGIVQDIEDEASNNVDHDYVYPL
22–47	FAM-VQDIEDEASNNVDHDYVYPLPENMVY